

Optical Testing and Metrology III: Recent Advances in Industrial Optical Inspection

C. P. Grover
Chair/Editor

8-13 July 1990
San Diego, California



Volume 1332

Part Two of Two Parts

PROCEEDINGS
 SPIE—The International Society for Optical Engineering

Optical Testing and Metrology III: Recent Advances in Industrial Optical Inspection

C. P. Grover
Chair/Editor

8–13 July 1990
San Diego, California

Sponsored by
SPIE—The International Society for Optical Engineering

Published by
SPIE—The International Society for Optical Engineering
P.O. Box 10, Bellingham, Washington 98227-0010 USA



Volume 1332

Part Two of Two Parts

SPIE (Society of Photo-Optical Instrumentation Engineers) is a nonprofit society dedicated to advancement of optical and optoelectronic applied science and technology.



The papers appearing in this book comprise the proceedings of the meeting mentioned on the cover and title page. They reflect the authors' opinions and are published as presented and without change, in the interests of timely dissemination. Their inclusion in this publication does not necessarily constitute endorsement by the editors or by SPIE.

Please use the following format to cite material from this book:

Author(s), "Title of Paper," *Optical Testing and Metrology III: Recent Advances in Industrial Optical Inspection*, C. P. Grover, Editor, Proc. SPIE 1332, page numbers (1990).

Library of Congress Catalog Card No. 90-52826
ISBN 0-8194-0393-8

SPIE—The International Society for Optical Engineering
P.O. Box 10, Bellingham, Washington 98227-0010 USA
Telephone 206/676-3290 (Pacific Time) • Fax 206/647-1445

Copyright © 1990, The Society of Photo-Optical Instrumentation Engineers.

Copying of material in this book for sale or for internal or personal use beyond the fair use provisions granted by the U.S. Copyright Law is subject to payment of copying fees. The Transactional Reporting Service base fee for this volume is \$2.00 per article and should be paid directly to Copyright Clearance Center, 27 Congress Street, Salem, MA 01970. For those organizations that have been granted a photocopy license by CCC, a separate system of payment has been arranged. The fee code for users of the Transactional Reporting Service is 0-8194-0393-8/90/\$2.00.

Individual readers of this book and nonprofit libraries acting for them are permitted to make fair use of the material in it, such as to copy an article for teaching or research, without payment of a fee. Reproduction or systematic or multiple reproduction of any material in this book (including abstracts) is prohibited except with the permission of SPIE and one of the authors.

Permission is granted to quote excerpts from articles in this book in other scientific or technical works with acknowledgment of the source, including the author's name, the title of the book, SPIE volume number, page number(s), and year. Reproduction of figures and tables is likewise permitted in other articles and books provided that the same acknowledgment of the source is printed with them, permission of one of the original authors is obtained, and notification is given to SPIE.

In the case of authors who are employees of the United States government, its contractors or grantees, SPIE recognizes the right of the United States government to retain a nonexclusive, royalty-free license to use the author's copyrighted article for United States government purposes.

Printed in the United States of America.

OPTICAL TESTING AND METROLOGY III:
RECENT ADVANCES IN INDUSTRIAL OPTICAL INSPECTION

Volume 1332

CONTENTS

Conference Committee	ix
Introduction	xi

Part One

SESSION 1	TESTING OF OPTICAL COMPONENTS AND SYSTEMS	
1332-01	Absolute measurement of spherical surfaces (Invited Paper) K. Creath, J. C. Wyant, WYKO Corp.	2
1332-02	High-precision interferometric testing of spherical mirrors with long radius of curvature K. R. Freischlad, M. Küchel, W. Wiedmann, W. Kaiser, M. Mayer, Carl Zeiss (FRG).	8
1332-03	Real-time wavefront measurement with $\lambda/10$ fringe spacing for the optical shop K. R. Freischlad, M. Küchel, K. Schuster, U. Wegmann, W. Kaiser, Carl Zeiss (FRG).	18
1332-36	System calibration and part alignment for inspection of 2-D electronic circuit patterns A. A. Rodriguez, IBM Corp.; J. R. Mandeville, F. Y. Wu, IBM/Thomas J. Watson Research Ctr. ...	25
1332-04	Simple test for the 90 degree angle in prisms D. Malacara, Univ. of Rochester (Mexico); R. Flores, Ctr. de Investigaciones en Optica, A.C. (Mexico).	36
1332-05	Set of two 45° - 90° - 45° prisms equivalent to the Fresnel rhomb M. V. Murty, R. P. Shukla, K. V. Appa Rao, Bhabha Atomic Research Ctr. (India).	41
1332-06	Focal length measurement using diffraction at a grating R. S. Sirohi, H. Kumar, N. K. Jain, Indian Institute of Technology (India).	50
1332-08	Automatic inspection technique for optical surface flaws G. Yang, W. Gao, S. Cheng, Zhejiang Univ. (China).	56
SESSION 2	TESTING OF ASPHERIC AND GENERALIZED SURFACES	
1332-09	Aspheric surface testing techniques (Invited Paper) H. P. Stahl, Stahl Optical Systems and Rose-Hulman Institute of Technology.	66
1332-10	Interferometer for testing aspheric surfaces with electron-beam computer-generated holograms T. Gemma, M. Hideshima, M. Taya, N. Watanabe, Topcon Corp. (Japan).	77
1332-59	Rigorous optical theory of the D Sight phenomenon (Special Paper) R. L. Reynolds, O. L. Hageniers, Diffracto Ltd. (Canada).	85
1332-13	Optical aspheric surface profiler using phase shift interferometry K. Sasaki, A. Ono, Toshiba Corp. (Japan).	97
1332-14	Aspheric testing using null mirrors M. V. Mantravadi, V. Kumar, R. J. von Handorf, Northrop Corp.	107
1332-94	Scattering measurements of optical coatings in high-power lasers (Proceedings only) Y. Chen, Shanghai Institute of Optics and Fine Mechanics (China).	115
SESSION 3	HOLOGRAPHY AND HOLOGRAPHIC INTERFEROMETRY	
1332-16	Application of real-time holographic interferometry in the nondestructive inspection of electronic parts and assemblies C. P. Wood, J. D. Trolinger, MetroLaser.	122

(continued)

OPTICAL TESTING AND METROLOGY III:
RECENT ADVANCES IN INDUSTRIAL OPTICAL INSPECTION

Volume 1332

1332-17	White-light transmission holographic interferometry using chromatic corrective filters C. P. Grover, National Research Council Canada (Canada).	132
1332-18	TV holography and image processing in practical use (Invited Paper) O. J. Løkberg, S. Ellingsrud, Norwegian Institute of Technology (Norway); E. Vikhagen, Foundation of Scientific and Industrial Research (Norway).	142
1332-19	Holographic instrumentation for monitoring crystal growth in space J. D. Trolinger, MetroLaser; R. B. Lal, A. K. Batra, Alabama A&M Univ.	151
1332-102	Holotag: a novel holographic label (Invited Paper) O. D. Soares, L. M. Bernardo, M. I. Pinto, F. V. Morais, Univ. do Porto (Portugal).	166
1332-20	Van der Lugt optical correlation for the measurement of leak rates of hermetically sealed packages C. M. Fitzpatrick, Electro Optic Consulting Services; E. P. Mueller, Ctr. for Devices and Radiological Health/FDA.	185
1332-21	Holographic interferometry in corrosion studies of metals: I. Theoretical aspects K. J. Habib, Kuwait Institute for Scientific Research (Kuwait).	193
1332-22	Holographic interferometry in corrosion studies of metals: II. Applications K. J. Habib, Kuwait Institute for Scientific Research (Kuwait).	205
1332-23	Numerical investigation of effect of dynamic range and nonlinearity of detector on phase-stepping holographic interferometry Q. Fang, X. Luo, Y. Tan, Xi'an Jiaotong Univ. (China).	216
SESSION 4	HOLOGRAPHY AND PHASE CONJUGATION	
1332-24	Holography with a single picosecond pulse (Invited Paper) N. H. Abramson, Royal Institute of Technology (Sweden).	224
1332-25	Holographic measurement of the angular error of a table moving along a slideway K. Matsuda, K. Tenjinbayashi, Mechanical Engineering Lab. (Japan).	230
1332-26	Optical testing by dynamic holographic interferometry with photorefractive crystals and computer image processing V. I. Vlad, D. Popa, Institute of Atomic Physics (Romania); M. P. Petrov, A. Kamshilin, Physics-Technical Institute (Romania).	236
1332-27	Optical phase-conjugate resonators, bistabilities, and applications (Invited Paper) P. Venkateswarlu, M. Dokhanian, P. C. Sekhar, M. C. George, H. Jagannath, Alabama A&M Univ.	245
1332-28	Phase-conjugate interferometry by using dye-doped polymer films K. Nakagawa, C. Egami, Muroran Institute of Technology (Japan); T. Suzuki, Kowa Co. Ltd. (Japan); H. Fujiwara, Muroran Institute of Technology (Japan).	267
1332-29	Phase-conjugate Twyman-Green interferometer for testing conicoidal surfaces R. P. Shukla, M. Dokhanian, P. Venkateswarlu, M. C. George, Alabama A&M Univ.	274
1332-30	Nondestructive testing of printed circuit board by phase-shifting interferometry (Proceedings only) Y. Lu, L. Jiang, L. Zou, X. Zhao, J. Sun, Harbin Institute of Technology (China).	287
SESSION 5	IMAGE METROLOGY AND 3-D VISION	
1332-31	Industrial applications of optical fuzzy syntactic pattern recognition H. J. Caulfield, Univ. of Alabama in Huntsville.	294
1332-32	Absolute range measurement system for real-time 3-D vision C. M. Wood, M. M. Shaw, D. M. Harvey, C. A. Hobson, M. J. Lalor, J. T. Atkinson, Liverpool Polytechnic (UK).	301

OPTICAL TESTING AND METROLOGY III:
RECENT ADVANCES IN INDUSTRIAL OPTICAL INSPECTION

Volume 1332

1332-33	New stereo laser triangulation device for specular surface inspection M. Samson, M. L. Dufour, National Research Council Canada (Canada).....	314
1332-34	Visual inspection system using multidirectional 3-D imager T. Koezuka, Y. Kakinoki, S. Hashinami, M. Nakashima, Fujitsu Labs. Ltd., Atsugi (Japan).	323
1332-35	Real-time edge extraction by active defocusing Y. Y. Hung, Q. Zhu, D. Shi, S. Tang, Oakland Univ.....	332
1332-101	3-D camera based on differential optical absorbance R. Houde, D. Laurendeau, D. Poussart, Laval Univ. (Canada).	343
1332-37	Algorithm for the generation of look-up range table in 3-D sensing X. Su, W. Zhou, Sichuan Univ. (China).	355
1332-38	Information extracting and application for the combining objective speckle and reflection holography Z. Cao, F. Chen, Tongji Univ. (China).	358
SESSION 6 FIBER OPTIC AND LASER SENSING I		
1332-39	Surface inspection using optical fiber sensor M. Abe, S. Ohta, M. Sawabe, Mitutoyo Corp. (Japan).	366
1332-41	Fiber optic smart structures: structures that see the light (Invited Paper) R. M. Measures, Univ. of Toronto and Ontario Laser and Lightwave Research Ctr. (Canada).	377
1332-42	Near real-time operation of a centimeter-scale distributed fiber sensing system B. K. Garside, Opto-Electronics Inc. (Canada).	399
1332-43	Geometric measurement of optical fibers with pulse-counting method Q. Nie, J. C. Nelson, S. C. Fleming, Univ. of Leeds (UK).	409
1332-44	Interferometric fiber optic sensors for use with composite materials R. M. Measures, T. Valis, K. Liu, W. D. Hogg, S. M. Ferguson, E. Tapanes, Univ. of Toronto and Ontario Laser and Lightwave Research Ctr. (Canada).	421
1332-45	Fiber optic damage detection for an aircraft leading edge R. M. Measures, M. LeBlanc, W. D. Hogg, K. McEwen, B. Park, Univ. of Toronto and Ontario Laser and Lightwave Research Ctr. (Canada).	431
SESSION 7 FIBER OPTIC AND LASER SENSING II		
1332-46	Low-cost fiber optic sensing systems using spatial division multiplexing (Invited Paper) B. E. Paton, Dalhousie Univ. (Canada).	446
1332-47	Two-dimensional micropattern measurement using precision laser beam scanning H. Fujita, Citizen Watch Co., Ltd. (Japan).	456
1332-49	GRIN fiber lens connectors C. Gómez-Reino, J. Liñares, Univ. de Santiago de Compostela (Spain).	468
1332-50	Laser-based triangulation techniques in optical inspection of industrial structures T. A. Clarke, K. T. Grattan, N. E. Lindsey, City Univ. (UK).	474
1332-51	Application of fiber optic sensors in pavement maintenance M. Shadaram, A. Solehjoui, S. Nazarian, Univ. of Texas/El Paso.	487
1332-52	Laser ultrasonics: generation and detection considerations for improved signal-to-noise ratio J. W. Wagner, J. B. Deaton, Jr., A. D. McKie, J. B. Spicer, Johns Hopkins Univ.	491

(continued)

OPTICAL TESTING AND METROLOGY III:
RECENT ADVANCES IN INDUSTRIAL OPTICAL INSPECTION

Volume 1332

Part Two

SESSION 8	OPTICAL PROFILING OF SURFACE MICROTOPOGRAPHY	
1332-55	Effects of the nonvanishing tip size in mechanical profile measurements E. L. Church, U.S. Army Research & Development Command; P. Z. Takacs, Brookhaven National Lab.	504
1332-56	Three-dimensional nanoprofilng of semiconductor surfaces P. C. Montgomery, J. B. Fillard, N. Tchandjou, M. S. Ardisasmita, Univ. des Sciences et Techniques du Languedoc (France).	515
1332-105	Optical surface microtopography using phase-shifting Nomarski microscope (Special Paper) W. Shimada, T. Sato, T. Yatagai, Univ. of Tsukuba (Japan).	525
1332-57	Laser moire topography for 3-D contour measurement T. Matsumoto, Y. Kitagawa, Hyogo Prefecture Industrial Research Institute (Japan); M. Adachi, Kanazawa Univ. (Japan); A. Hayashi, Kobe City College of Technology (Japan).	530
1332-58	Nomarski viewing system for an optical surface profiler J. R. Bietry, R. A. Auriemma, T. C. Bristow, E. Merritt, Chapman Instruments.	537
1332-60	Surface microtopography of thin silver films M. F. Costa, J. B. Almeida, Univ. do Minho (Portugal).	544
SESSION 9	SUBMICRON DISTANCE METROLOGY	
1332-61	Design criteria of an integrated optics microdisplacement sensor A. d'Alessandro, M. De Sario, A. D'Orazio, V. Petruzzelli, Univ. di Bari (Italy).	554
1332-62	Laser-scanning tomography and related dark-field nanoscopy method P. C. Montgomery, P. Gall, M. S. Ardisasmita, M. Castagné, J. Bonnafé, J. B. Fillard, Univ. des Sciences et Techniques du Languedoc (France).	563
1332-63	Super-accurate positioning technique using diffracted moire signals Y. Takada, Y. Uchida, Y. Akao, J. Yamada, Aichi Institute of Technology (Japan); S. Hattori, Nagoya Industrial Science Research Institute (Japan).	571
1332-64	Moire displacement detection by the photoacoustic technique K. Hane, S. Watanabe, T. Goto, Nagoya Univ. (Japan).	577
1332-65	Displacement measurement using grating images detected by CCD image sensor K. Hane, Nagoya Univ. (Japan); C. P. Grover, National Research Council Canada (Canada).	584
1332-66	Noncontact technique for the measurement of linear displacement using chirped diffraction gratings W. B. Spillman, Jr., Simmonds Precision; P. L. Fuhr, Univ. of Vermont.	591
1332-67	Interferometric measurement of in-plane motion M. Hercher, G. J. Wyntjes, Optra, Inc.	602
1332-68	Automatic mask-to-wafer alignment and gap control using moire interferometry V. T. Chitmis, S. Kowsalya, A. Rashmi, A. K. Kanjilal, R. Narain, National Physical Lab. (India). ..	613
SESSION 10	NOVEL INTERFEROMETRIC METROLOGY DEVICES	
1332-70	Interference phenomenon with correlated masks and its application C. P. Grover, K. Hane, National Research Council Canada (Canada).	624
1332-71	Multichannel chromatic interferometry: metrology applications (Invited Paper) G. M. Tribillon, Univ. de Franche-Comté (France); J. Calatroni, Univ. Simon Bolivar (Venezuela); P. Sandoz, Univ. de Franche-Comté (France).	632

OPTICAL TESTING AND METROLOGY III:
RECENT ADVANCES IN INDUSTRIAL OPTICAL INSPECTION

Volume 1332

1332-69	Fringe-scanning moire system using a servo-controlled grating H. Kurokawa, N. Ichikawa, Mechanical Engineering Lab. (Japan); N. Yajima, Institute of Space and Astronautical Science (Japan).....	643
1332-72	New Zeiss interferometer (Special Paper) M. Küchel, Carl Zeiss (FRG).	655
1332-73	Software concept for the new Zeiss interferometer B. Doerband, W. Wiedmann, U. Wegmann, W. Kübler, K. R. Freischlad, Carl Zeiss (FRG).	664
1332-103	New technique for multiplying the isoclinic fringes M. Wen, G. T. Liu, Tsinghua Univ. (China).	673
SESSION 11 FRINGE ANALYSIS AND PHASE MEASUREMENT		
1332-76	Review of interferogram analysis methods (Invited Paper) D. Malacara, Univ. of Rochester (Mexico).....	678
1332-77	Automatic, high-resolution analysis of low-noise fringes G. D. Lassahn, EG&G Idaho, Inc.	690
1332-78	Three-dimensional surface inspection using interferometric grating and 2-D FFT-based technique Y. Y. Hung, S. Tang, Q. Zhu, Oakland Univ.	696
1332-80	Review of phase-measuring interferometry (Invited Paper) H. P. Stahl, Stahl Optical Systems and Rose-Hulman Institute of Technology.	704
1332-81	White-light moire phase-measuring interferometry H. P. Stahl, Stahl Optical Systems and Rose-Hulman Institute of Technology.	720
1332-82	New phase measurement for nonmonotonical fringe patterns S. Tang, Y. Y. Hung, Q. Zhu, Oakland Univ.	731
1332-83	Synchronous phase-extraction technique and its applications Y. Y. Hung, S. Tang, G. Jin, Q. Zhu, Oakland Univ.	738
SESSION 12 SPECIALIZED TECHNIQUES AND APPLICATIONS I		
Stress, Strain, and Shockwaves		
1332-84	Optical techniques for determination of normal shock position in supersonic flows for aerospace applications G. Adamovsky, NASA/Lewis Research Ctr.; J. G. Eustace, John Carroll Univ.	750
1332-86	Two-dimensional surface strain measurement based on a variation of Yamaguchi's laser-speckle strain gauge J. P. Barranger, NASA/Lewis Research Ctr.	757
1332-85	Estimation of plastic strain by fractal (Proceedings only) Y. Z. Dai, F. Chiang, SUNY/Stony Brook.	767
1332-87	Photoelastic transducer for high-temperature applications (Proceedings only) A. S. Redner, Strainoptic Technologies, Inc.; G. Adamovsky, NASA/Lewis Research Ctr.; L. N. Wesson, Aurora Optics, Inc.	775
Refractometry		
1332-95	Simultaneous measurement of refractive index and thickness of thin film by polarized reflectances T. Kihara, K. Yokomori, Ricoh Co. Ltd. (Japan).....	783

OPTICAL TESTING AND METROLOGY III:
RECENT ADVANCES IN INDUSTRIAL OPTICAL INSPECTION

Volume 1332

	Process Control	
1332-88	Study of oxidization process in real time using speckle correlation M. Muramatsu, G. H. Guedes, Univ. of São Paulo (Brazil); K. Matsuda, T. H. Barnes, Mechanical Engineering Lab. (Japan).	792
1332-89	Application of speckle metrology at a nuclear waste repository E. Conley, J. Genin, New Mexico State Univ.	798
1332-90	Study of microbial growth I: by diffraction G. T. Williams, R. D. Bahuguna, H. Arteaga, E. N. Le Joie, San Jose State Univ.	802
1332-107	Study of microbial growth II: by holographic interferometry R. D. Bahuguna, G. T. Williams, I. K. Pour, R. Raman, San Jose State Univ.	805
1332-91	Basic use of acoustic speckle pattern for metrology and sea waves study D. He, East China Institute of Technology (China); M. He, Qingdao Univ. of Oceanography (China).	808
1332-106	Optical three-dimensional sensing for measurement of bottomhole pattern W. Su, Southwestern Petroleum Institute (China); X. Su, Sichuan Univ. (China).	820
SESSION 13	SPECIALIZED TECHNIQUES AND APPLICATIONS II	
	Surface Roughness	
1332-92	Light scattered by coated paper E. Marx, J. F. Song, T. V. Vorburger, T. R. Lettieri, National Institute of Standards and Technology.	826
1332-93	Statistical properties of intensity fluctuations produced by rough surfaces under the speckle pattern illumination T. Yoshimura, K. Fujiwara, E. Miyazaki, Kobe Univ. (Japan).	835
1332-11	Applications of diamond-turned null reflectors for generalized aspheric metrology J. T. McCann, Optical Filter Corp.	843
	Dynamic Measurement	
1332-97	Measurement of fluid velocity fields using digital correlation techniques D. R. Matthys, Marquette Univ.; J. A. Gilbert, Univ. of Alabama in Huntsville; J. T. Puliparambil, Marquette Univ.	850
1332-98	Studies on laser dynamic precision measurement of fine-wire diameters L. Bao, F. Chen, S. Wu, J. Xu, Z. Guan, Hefei Univ. of Technology (China).	862
	Video and E-O Systems	
1332-99	Measurement of interfacial tension by automated video techniques V. A. Deason, R. L. Miller, A. D. Watkins, M. B. Ward, K. B. Barrett, Idaho National Engineering Lab.	868
1332-100	Design parameters of an EO sensor L. S. Tanwar, P. C. Jain, National Physical Lab. (India); H. Kunzmann, Physikalisch-Technische Bundesanstalt (FRG).	877
	Addendum.	883
	Author Index.	884

Effects of the non-vanishing tip size in mechanical profile measurements

E. L. Church
USA ARDEC, Dover NJ 07801-5000

P. Z. Takacs
Brookhaven National Laboratory, Upton NY 11973-5000

ABSTRACT

The high-spatial-frequency behavior of mechanical-profiling instruments is determined principally by the non-linear geometrical interaction between the stylus tip and the surface irregularities. There is considerable interest in the nature of this interaction and its effects in practical applications. This paper explores these issues analytically and presents a variety of results with emphasis on the frequency-domain description. Smooth surfaces are treated by perturbation theory and are found to be roughened by tip-size effects, while rough surfaces are smoothed. In lieu of closed form results for rough surfaces, we offer a simple conjecture regarding the nature of tip-size distortions and the maximum useable spatial frequency.

1. INTRODUCTION

All profile-measuring techniques are band-width limited; that is, they are sensitive to only a limited range of surface frequencies f . Optical measurements are generally linear over their operating range, and it is straight forward to determine their extreme band-width limits in terms of system parameters. In the case of Wyko-like measurements [1-4]:

$$\frac{1}{L} < f_{\text{OPT}} < \frac{1}{\lambda} \quad (1)$$

where L is the trace length and λ is the wavelength of the radiation used (HeNe or thereabouts). This last means that the highest accessible spatial frequency is of the order of $1 \mu\text{m}^{-1}$.

The corresponding length parameters which determine the band-width limits of mechanical-profiling instruments are the trace length L and the radius of the stylus tip, R . In contrast with optical techniques, mechanical measurements are inherently non-linear at high spatial frequencies and the upper frequency limit of their bandpass is not simply $1/R$, but some more complicated function of both R and surface-finish parameters, which we denote by the collective symbol α :

$$\frac{1}{L} < f_{\text{MECH}} < F(R, \alpha) \quad (2)$$

Since tip dimensions can be made as small as $R \sim 0.1 \mu\text{m}$ there is the possibility of breaking the visible-light barrier using mechanical-stylus measurements; but how well and by how much depends on the nature of the non-linear geometrical interaction between the stylus tip and the surface contour.

Tip-size effects are easily calculated for specific surface shapes. For a sinusoidal profile of amplitude A , for example, this leads to the rule of thumb [5-7]:

$$F(R, \alpha) \approx \frac{1}{2\pi\sqrt{AR}} \quad (3)$$

Note that this result varies as $R^{-1/2}$ rather than R^{-1} , which reflects the non-linear nature of the measurement process. Later results involve even more complicated dependences on the tip size.

In this paper we address the more general problem of determining the effects of the tip size on the finish parameters of randomly rough surfaces, and, in particular, their power spectral densities $S(f)$. Little, if any, work appears to have been done in this area [8,9].

As a first step we consider the canonical problem of a circle of radius R rolling over a one-dimensional randomly-rough surface with the profile $Z(x)$. The measured profile is then defined as the locus of the lowest point on the circle.

2. SURFACE STATISTICS

The discussion of tip-size effects involves three surface parameters: σ , μ and γ ; the rms (root-mean-square) values of the profile height, slope and curvature:

$$\begin{pmatrix} \sigma^2 \\ \mu^2 \\ \gamma^2 \end{pmatrix} = \begin{pmatrix} \langle Z^2 \rangle \\ \langle (dZ/dx)^2 \rangle \\ \langle (d^2Z/dx^2)^2 \rangle \end{pmatrix} \quad (4)$$

These may be written in terms of the moments of the profile power spectrum, $S(f)$:

$$\begin{pmatrix} \sigma^2 \\ \mu^2 \\ \gamma^2 \end{pmatrix} = \int_0^\infty df S(f) \cdot \begin{pmatrix} (2\pi f)^0 \\ (2\pi f)^2 \\ (2\pi f)^4 \end{pmatrix} \quad (5)$$

or equivalently, in terms of the zeroth, second and fourth derivatives of the profile covariance function at zero lag [10,11].

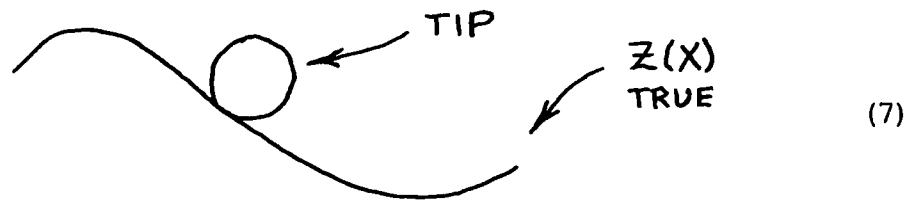
We also define a new quantity, the "rms radius of curvature" $\rho \triangleq 1/\gamma$, for comparison with the tip radius. This enables us to distinguish two limiting cases: $R \ll \rho$ which we call the sharp-tip limit, and $R \gg \rho$ which we call the blunt-tip limit.

3. SHARP-TIP LIMIT

In this case

$$R \ll \rho_{\text{TRUE}} \quad (6)$$

and the tip rides over the surface so:



That is, the bottom of the tip tracks the surface smoothly but experiences an offset which depends on the surface slope [3,4]:

$$Z(X)_{\text{MEASURED}} = Z(X)_{\text{TRUE}} + \frac{R}{2} \left(\frac{dz}{dx} \right)^2 + \dots \quad (8)$$

This shows that tip-size effects roughen the measured profile in this limit.

Equation 8 can be rewritten in the frequency domain as

$$S(f)_{\text{MEASURED}} = S(f)_{\text{TRUE}} + \frac{1}{4} (2\pi)^4 R^2 \int_{-\infty}^{+\infty} dg g^2 (g-f)^2 S(1g)_{\text{TRUE}} S(1g-f)_{\text{TRUE}} + \dots \quad (9)$$

where the second term on the right is the tip-size correction. Using this, we can calculate the effects on the finish parameters using Eq 5. For example,

$$\sigma^2_{\text{MEASURED}} = \sigma^2_{\text{TRUE}} + \frac{1}{2} R^2 \mu^4_{\text{TRUE}} + \dots \quad (10)$$

If we require that the second term be small relative to the first, we find

$$R \ll \sqrt{2} \left(\frac{\sigma}{\mu^2} \right)_{\text{TRUE}} \quad (11)$$

which gives an additional requirement on the tip radius in terms of the moment parameters (cf Eq 6).

The most important use of Eq 9, however, lies in the fact that it provides a means for determining the maximum measurable frequency (Eq 2) by imposing conditions on the relative importance of the second term relative to the first. This procedure is illustrated below.

3.1 Sinusoidal profile

For the sinusoid

$$z_{\text{TRUE}}(x) = A \sin \left(2\pi \frac{x}{d} \right) \quad (12)$$

we have

$$\rho_{\text{TRUE}} = \frac{\sqrt{2}}{(2\pi)^2} \cdot \frac{d^2}{A} \quad (13)$$

Eq 9 then gives

$$S_{\text{MEASURED}}(f) = \frac{1}{2} A^2 \delta \left(f - \frac{1}{d} \right) + \frac{1}{8} \left(\frac{R}{\rho} \right)^2 \delta \left(f - \frac{2}{d} \right) + \dots \quad (14)$$

The first term is the spectrum of the true profile and the second, which appears at twice the original frequency, is the first-order tip correction. If we define the maximum allowable spectral distortion to occur when the second term is 1/16-th the first, we obtain a condition on the radius which is precisely that in Eq 3.

3.2 Rectangular spectrum

Here we consider the random profile whose spectrum is band-width-limited white noise; that is

$$S(f) = K \cdot U \left(\frac{f}{f_0} \right) \quad (15)$$

where K and f_0 are constants and $u(x)$ is a step function: $u(x) = 1$ for $0 \leq x \leq 1$ and zero otherwise. In this case

$$\rho_{\text{TRUE}} = \frac{1}{(2\pi)^2} \sqrt{\frac{5}{K f_0^5}} \quad (16)$$

and

$$S(f)_{\text{MEASURED}} = K \left[U\left(\frac{f}{f_0}\right) + \left(\frac{R}{\rho}\right)^2 \left\{ \frac{12 - 30x + 20x^2 - x^5}{24} \right\} U\left(\frac{f}{2f_0}\right) + \dots \right] \quad (17)$$

where $x = f/f_0$. Note that the second term extends to twice the frequency of the true spectrum.

The curly bracket has a maximum of 0.5 at $x = 0$ and reaches a secondary maximum of 0.1972 at $x = 1.628$ before vanishing at $x = 2$. This means that the sharp-tip condition, Eq 6, is sufficient in itself to ensure the smallness of the correction in this example.

3.3 Gaussian spectrum

Here

$$S(f)_{\text{TRUE}} = 2\sqrt{\pi} \sigma^2 \ell e^{-(\pi \ell f)^2} \quad (18)$$

where ℓ is the 1/e correlation length. In this case

$$\rho_{\text{TRUE}} = \frac{1}{\sqrt{12}} \frac{\ell^2}{\sigma} \quad (19)$$

and the measured spectrum is

$$S(f)_{\text{MEASURED}} = S(f)_{\text{TRUE}} \left[1 + \left(\frac{R}{\rho}\right)^2 \left\{ \frac{3 - 2x^2 + x^4}{24\sqrt{2}} e^{+x^2/2} \right\} + \dots \right] \quad (20)$$

where $x = \pi \ell f$.

This curly bracket increases monotonically at high frequencies, and the tip correction eventually dominates the true spectrum. In this case, then, the sharp-tip

condition alone is not sufficient to ensure the smallness of the correction and we must impose an additional constraint on the maximum allowable frequency.

For example, if $R = 0.1 \varphi$ and we require that the second term in Eq 20 be less than 0.1 the first, f must be less than $0.745/\ell$; a result which is in the form of Eq 2, where the R dependence is implicit in the numerical factor.

4. HUNT-TIP LIMIT

This means

$$R \gg \varphi_{\text{TRUE}} \quad (21)$$

where φ may be non vanishing or zero [11]. In this limit the tip may follow the low-frequency contour of the surface but rides over the high-frequency variations:



The measured profile then has an asymmetric, cloud-like appearance; with rounded peaks having a radius of the order of that of the tip separated by cusp-shaped valleys:



In this limit the tip smooths the surface by "filtering-out" high frequencies. At the same time it adds an $f(-4)$ component to the measured spectrum due to the discontinuities in slope at the tips of the cusps [10,12]. In the limit one might expect the spectrum to be dominated by this $f(-4)$ component.

5. COMMENTS AND CONJECTURE

5.1 Comments

The discussion above exploits physical idea that we can distinguish two extreme forms of behavior by comparing the stylus tip size with the rms curvature of the surface. In either regime one can, in principle at least, determine an allowable upper frequency based on a spectrum-based criterion of acceptability. We end up then, with two conditions: a configuration-space one on the tip radius and a

frequency-space one on the maximum frequency. From this point of view our hoped-for limit in Eq 2 turns out to be double barreled. This is inconvenient.

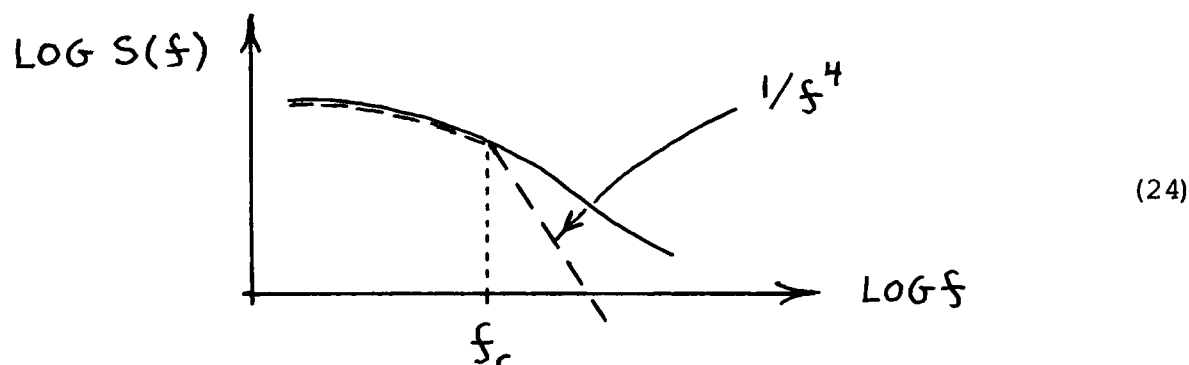
Another disadvantage of this approach is that it requires a-priori knowledge of the true spectrum which may not be available. Also, at this point at least, we have no detailed way of handling the problem except in the sharp-tip limit, where we have used a perturbation approach.

We would like to reformulate the problem in a way that does not involve the surface curvature explicitly, and determine the conditions for the useable frequency range directly in terms of the spectral parameters rather than its moments. For this we consider an ad-hoc procedure based on the above ideas which we state below in the form of a conjecture [3,4]. We offer this as an interim operating scheme and a target for future improvements.

5.2 Conjecture

"The spectrum of the measured profile is the same as that of the original profile up to a critical frequency, f_c , above which it falls off as f^{-4} . This frequency is determined by evaluating the moment integral of the mean-square profile curvature (Eq 5) between zero and f_c , multiplying the result by a constant of order unity, and setting the result equal to the mean-square curvature of the tip, $1/R^2$."

Graphically, this means:



where the solid line is the true spectrum, the dashed line is the measured spectrum, and f_c is the critical frequency.

Algebraically:

$$S_{\text{MEASURED}}(f) = S_{\text{MEASURED}}(f) \cdot U\left(\frac{f}{f_c}\right) + S_{\text{MEASURED}}(f_c) \left(\frac{f_c}{f}\right)^4 \cdot \left[1 - U\left(\frac{f}{f_c}\right)\right] \quad (25)$$

and f_c is defined implicitly by the equation

$$\frac{1}{R^2} = C \cdot (2\pi)^4 \int_0^{f_c} d f S_{\text{MEASURED}}(f) \cdot f^4 \quad (26)$$

where C is a constant of order unity.

This conjecture applies over the whole range of tip sizes. To establish the connection with the sharp-tip limit, note that in that case the right-hand side of Eq 26 approaches a finite value of C/ρ^2 as $f_c \rightarrow \infty$, and the conjecture then states that the measured spectrum will be totally unaffected providing

$$R < \rho/\sqrt{C} \quad (27)$$

as compared with Eq 6. If this inequality is not satisfied, Eq 26 leads to a finite value of the critical frequency, which may be taken as the upper limit of the undistorted spectrum; that is

$$F(R, \alpha) = f_c \quad (28)$$

To illustrate the application of Eqs 25 and 26 we evaluate them below for the spectral shapes considered in the previous section. Further examples are given in the Appendix.

5.3.1 Sinusoidal profile

If the tip radius satisfies Eq 27, f_c will be infinite and Eq 25 says that the measured spectrum will be unaffected. If Eq 27 is not satisfied, $f_c = 1/d$, and Eq 25, when reinterpreted for this special case of a deterministic profile, predicts that the measured spectrum will be a series of inverse-fourth-power harmonics corresponding to a regular series of parabolic cusps of depth $d^2/8R$ [12]. The dividing line between these two regimes lies at

$$f_c = \left[\frac{2}{C} \right]^{1/4} \cdot \frac{1}{2\pi \sqrt{AR}} \quad (29)$$

which is the same as Eq 3 except for the fourth-root factor, which is expected to be of order unity.

5.3.2 Rectangular spectrum

Here the spectrum will be unaffected up to

$$f_c = \frac{1}{2\pi} \left[\frac{10\pi}{C\kappa R^2} \right]^{1/5} \quad (30)$$

If this is less than f_0 , Eq 25 says that a portion the high-frequency end of the measured spectrum will be cut off and replaced by an inverse quartic tail, but if it is greater than f_0 the measured profile will be unaffected. In contrast, perturbation theory predicts a small high-frequency contribution out to $2f_0$ (Eq 17).